Exhibit 606

Cardiac side effects of RNA-based SARS-CoV-2 vaccines: Hidden cardiotoxic effects of mRNA-1273 and BNT162b2 on ventricular myocyte function and structure

https://bpspubs.onlinelibrary.wiley.com/doi/epdf/10.1111/bph.16262

Received: 25 May 2023 | Revised: 16 July 2023 | Accepted: 3 August 2023

DOI: 10.1111/bph.16262

RAPID COMMUNICATION

Cardiac side effects of RNA-based SARS-CoV-2 vaccines: Hidden cardiotoxic effects of mRNA-1273 and BNT162b2 on ventricular myocyte function and structure

Rolf Schreckenberg[1] | Nadine Woitasky[1] | Nadja Itani[1] | Laureen Czech[1] | Péter Ferdinandy[2,3] | Rainer Schulz[1]

[1]Institute of Physiology, Faculty of Medicine, Justus-Liebig University, Gießen, Germany

[2]Department of Pharmacology and Pharmacotherapy, National Heart Laboratory, Semmelweis University, Budapest, Hungary

[3]Pharmahungary Group, Szeged, Hungary

Correspondence
Rolf Schreckenberg, Institute of Physiology, Faculty of Medicine, Justus-Liebig University, Aulweg 129, D-35392 Gießen, Germany.
Email: rolf.schreckenberg@physiologie.med.uni-giessen.de

Funding information
National Research, Development and Innovation Office of Hungary, Grant/Award Numbers: 2020-1.1.6-JÖVŐ-2021-00013, RRF-2.3.1-21-2022-00003; EU Horizon 2020 project COVIRNA, Grant/Award Number: #101016072

Abstract

Background and Purpose: To protect against SARS-CoV-2 infection, the first mRNA-based vaccines, Spikevax (mRNA-1273, Moderna) and Comirnaty (BNT162b2, Pfizer/Biontech), were approved in 2020. The structure and assembly of the immunogen—in both cases, the SARS-CoV-2 spike (S) glycoprotein—are determined by a messenger RNA sequence that is translated by endogenous ribosomes. Cardiac side-effects, which for the most part can be classified by their clinical symptoms as myo- and/or pericarditis, can be caused by both mRNA-1273 and BNT162b2.

Experimental Approach: As persuasive theories for the underlying pathomechanisms have yet to be developed, this study investigated the effect of mRNA-1273 and BNT162b2 on the function, structure, and viability of isolated adult rat cardiomyocytes over a 72 h period.

Key Results: In the first 24 h after application, both mRNA-1273 and BNT162b2 caused neither functional disturbances nor morphological abnormalities. After 48 h, expression of the encoded spike protein was detected in ventricular cardiomyocytes for both mRNAs. At this point in time, mRNA-1273 induced arrhythmic as well as completely irregular contractions associated with irregular as well as localized calcium transients, which provide indications of significant dysfunction of the cardiac ryanodine receptor (RyR2). In contrast, BNT162b2 increased cardiomyocyte contraction via significantly increased protein kinase A (PKA) activity at the cellular level.

Conclusion and Implications: Here, we demonstrated for the first time, that in isolated cardiomyocytes, both mRNA-1273 and BNT162b2 induce specific dysfunctions that correlate pathophysiologically to cardiomyopathy. Both RyR2 impairment and sustained PKA activation may significantly increase the risk of acute cardiac events.

KEYWORDS
BNT162b2, cardiac dysfunction, cardiac side effects, mRNA-1273, protein kinase A (PKA), ryanodine receptor (RyR2), SARS-CoV-2 spike (S) glycoprotein

Abbreviations: α-MHC, α-myosin heavy chain; $dL \cdot L^{-1}$ in %, relative cell shortening; F-actin, filamentous actin; ISO, isoprenaline; LNP, lipid nanoparticle; mRNA, messenger RNA; phalloidine-TRITC, phalloidine tetramethylrhodamine B isothiocyanate; PKA, protein kinase A; PM, Powell medium; RyR2, cardiac ryanodine receptor; SR, sarcoplasmic reticulum.

1 | INTRODUCTION

With the approval of the first mRNA-based vaccines, an effective preventive measure against symptomatic infection with SARS-Cov-2 was available just a few months after the start of the pandemic. mRNA technology is based on the concept of relocating the production of specific (foreign) antigens in the body cells of vaccinated persons, which promises to significantly reduce development and manufacturing times. The structure of the immunogen is determined by the sequence of messenger RNA (mRNA) that is protected from degradation by means of lipid nanoparticles (LNPs) and taken up by the cells as an LNP-mRNA complex by simple endocytosis (Teo, 2021).

Development, preclinical and clinical safety and efficacy testing, and emergency approval were realized in under 12 months for mRNA-1273 (Spikevax, Moderna) and BNT162b2 (Comirnaty, Pfizer/Biontech), both of which encode the identical **SARS-CoV-2 spike (S) glycoprotein**. While basic immunization with mRNA-1273 and BNT162b2 efficiently reduced hospitalization and mortality rates associated with SARS-CoV-2, approximately 4 months after the start of the vaccination campaigns, the incomplete cardiac safety testing and exploration of the adverse event profile resulted in the diagnosis of cardiac side effects, which based on their clinical symptoms have been predominantly classified as myocarditis, pericarditis, or a combination thereof (Butt et al., 2021; D'Angelo et al., 2021; Ferdinandy et al., 2019; Heymans & Cooper, 2022; Nyberg et al., 2022; Sun et al., 2022). It should be noted that cardiac safety issues of many therapeutic agents appears only in the late phase of clinical developments or during their clinical application, termed hidden cardiotoxicity (Ferdinandy et al., 2019).

Numerous studies have demonstrated a statistical association between mRNA-based vaccines and adverse cardiac events and have analysed risk as a function of age and sex (Buchan et al., 2022; Chua et al., 2022; Karlstad et al., 2022; Le Vu et al., 2022; Sharff et al., 2022). In the Kaiser Permanente Northwest study, the risk of perimyocarditis within 30 days of two mRNA injections was reported to be 1/2650 in male adolescents aged 12 to 17, and 1/1862 in the 18- to 24-year-old age group (Sharff et al., 2022). These data are consistent with findings from the Hong Kong study by Chua et al., who calculated an incidence of 37.32 (95% CI, 26.98–51.25) per 100 000 male adolescents (Chua et al., 2022). In the 'Nordic Cohort' study, the incidence rate was also determined separately for both vaccines, which was 3.3 times higher after the second vaccination dose for mRNA-1273 (excess events: 5.55 [95% CI, 3.70–7.39] vs. 18.39 [9.05–27.72]) (Karlstad et al., 2022). Data from France confirmed this risk ratio (8.1 [95% CI, 6.7–9.9] vs. 30 [21–43]) and the authors also cautioned that both myocarditis and pericarditis posed a substantial risk in all age groups and for both sexes (Le Vu et al., 2022).

Compared with BNT162b2, a vaccine dose of mRNA-1273 contains 3.3 times the amount of mRNA (100 μg vs. 30 μg), so based on empirical data, there may be a correlation between the incidence of myocardial alterations and the amount of mRNA used. Due to the large number of components involved, the number of mRNA copies used cannot be extrapolated one-to-one to the synthesis rate of the spike protein, but the significantly higher geometric mean titers of neutralizing antibodies after basic immunization with mRNA-1273 also indicate significantly higher concentrations of the spike protein (Khoury et al., 2021; Tyner et al., 2022).

A currently favoured theory about the underlying pathomechanisms of myocardial alterations is based on the possibility of immunological cross-reactions. Antibodies directed against epitopes of the spike protein as a result of vaccination could also react with epitopes of the α-myosin heavy chain (α-MHC) (Vojdania & Kharrazian, 2020). However, α-MHC is a sarcomeric protein expressed almost exclusively in atria and cannot interact directly with circulating antibodies because of its purely intracellular localization (Racanelli et al., 2011).

Autoantibodies against α-MHC can be detected in the course of various diseases of the myocardium; however, aetiology and pathogenetic mechanisms are still poorly understood, so that a causal contribution to cardiac symptoms cannot be confirmed at present (Kaya et al., 2012).

Rationale for rapid communication

- The present preclinical cardiac safety data point to the need for a reassessment of the risk–benefit ratio of RNA-based SARS-Cov-2 vaccines, given indication of their cardiotoxicity.

What is already known

- While mRNA-based SARS-Cov-2 vaccines can induce cardiac side effects, the underlying mechanisms are not understood.

What does this study add

- Both mRNA-1273 and BNT162b2 can induce disturbances to regular contractile function.
- However, the associated mechanisms are functionally and pathophysiologically distinct.

What is the clinical significance

- The findings support both the diagnosis and treatment of cardiac events following mRNA-based COVID vaccination.
- The results may provide an explanation for persistent cardiac symptoms in connection with post-COVID syndrome.

The application of mRNAs are administered as complexes with LNPs, the distribution of which in the organism has been studied with radio-labelled tracers over a period of 2 days in Wistar rats (SARS-CoV-2 mRNA Vaccine, report number: 185350, n.d.; Li et al., 2022). Because lipid particles can reach the myocardium from the injection site after only a few minutes, in this study we examined the direct effect of mRNA-1273 and BNT162b2 on the function, structure, and viability of isolated rat cardiomyocytes over a 72 h period. After isolation, cellular and molecular effects directly attributable to the intrinsic effect of the two mRNA vaccines can be studied on the serum-free incubated ventricular muscle cells. The absence of immunocompetent cells allows indirect influences due to possible antigen–antibody reactions to be excluded. Additionally, the human cardiomyocyte cell line, AC16, was used to demonstrate the uptake of LNP-mRNA complexes and the translation of the encoded spike protein in human cells of ventricular origin (see Figure 1 '*Study design*').

Our present findings show for the first time in the literature that left ventricular myocytes both from rat and human origin express the encoded spike protein after incubation with both mRNA-1273 and BNT162b2; functionally, both mRNAs induce disturbances to normal contractile function within 24 to 48 h of application, which, however, differ fundamentally with respect to their symptomatology as well as their respective pathomechanisms.

2 | METHODS

All animal care and experimental procedures complied with the Guide for the Care and Use of Laboratory Animals published by the US National Institute of Health (NIH Publication No. 85-23, revised 1996) and were approved by the animal welfare office of the Justus-Liebig-University Gießen, Germany (internal registration number

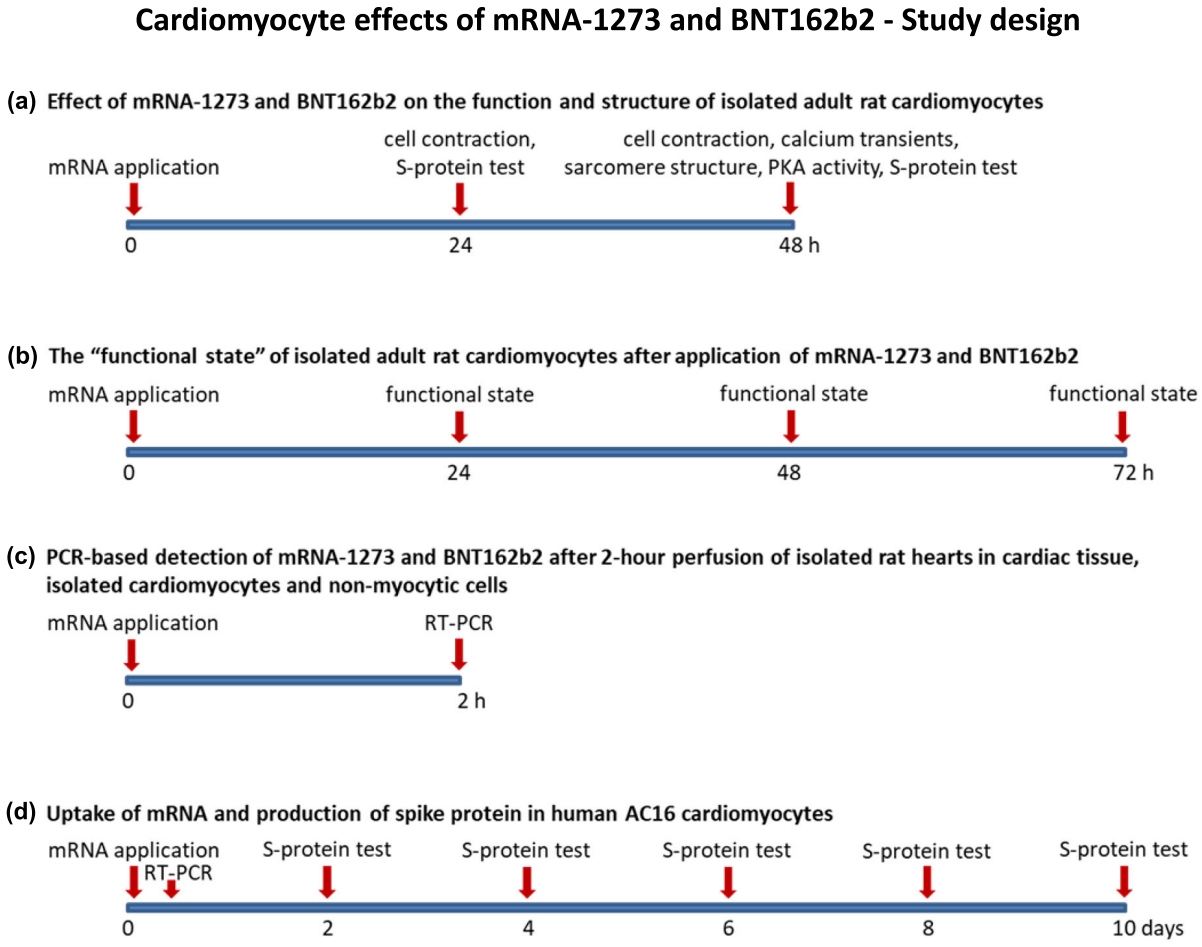

FIGURE 1 Plan of experiments to study effects of mRNA vaccines on cardiomyocytes. (a) The effect of mRNA-1273 and BNT162b2 on the function and structure of isolated rat cardiomyocytes was examined over a period of 48h. Both the cell fraction and supernatant were assayed for spike protein (S-protein) after 24h and 48h. (b) 24h, 48h, and 72h after application of mRNA-1273 and BNT162b2, isolated cardiomyocytes were stimulated in a blinded fashion using a 2 Hz electric field and assigned to one of the following categories: regular contraction, arrhythmic contraction, irregular contraction, no contraction, and rounded/hypercontracted. (c) mRNA uptake was assessed in rat hearts, after 2 h of Langendorff perfusion, in all sections of the left and right ventricular myocardium, septum, and both atria. Following the additional step of cell isolation, it was also possible to detect cell-specific uptake in cardiomyocytes and non-myocytic cells. (d) Using the human cardiomyocyte cell line AC16, it was possible to demonstrate both the efficient uptake of LNP-mRNA complexes and translation of the coded spike protein in human cells of ventricular origin.

772_M) and complied with EU directive 2010/63. Animal studies are reported in compliance with the ARRIVE guidelines (Percie du Sert et al., 2020) and with the recommendations made by the *British Journal of Pharmacology* (Lilley et al., 2020).

2.1 | Isolation and culture of ventricular cardiomyocytes

Left ventricular cardiomyocytes were isolated from the hearts of 3-month-old male Wistar (RjHan:WI) rats from Janvier Labs (Le Genest-Saint-Isle, France). Rats were anaesthetised, one at a time, in a desiccator (vol: 6 L), using 4%–5% **isoflurane** (IsoFlo 100% w/w, Zoetis Deutschland GmbH, Germany). After the eyelid reflex was extinguished, animals were killed by cervical dislocation.

Subsequently, hearts were perfused using the Langendorff technique at 37°C, first blood-free and then recirculating for 25 min with 50 ml of Powell medium (PM), 0.06% (w/v) type 2 collagenase (Worthington Biochemical Corp., USA), and 25 $\mu mol \cdot L^{-1}$ $CaCl_2$ (composition of PM in $mmol \cdot L^{-1}$: NaCl, 110; KH_2PO_4, 1.2; KCl, 2.6; $MgSO_4$, 1.2; HEPES, 25; and glucose, 10; adjusted to pH 7.4 and gassed with 5% CO_2–95% O_2). Mechanical comminution was followed by further enzymatic digestion for 5 min in 12 ml PM. The cell suspension was filtered through a 200-µm nylon mesh and separated from non-myocytic cells; purification and increase of calcium concentration from 0.2 to 0.5 $mmol \cdot L^{-1}$ were performed in three successive centrifugation steps. Subsequently, cells were taken up in 20 ml CCT cell culture medium (medium 199 with Earle's salts supplemented with 5 $mmol \cdot L^{-1}$ creatine, 5 $mmol \cdot L^{-1}$ L-carnitine, 5 $mmol \cdot L^{-1}$ taurine, 100 $IU \cdot ml^{-1}$ penicillin, and 100 $\mu g \cdot ml^{-1}$ streptomycin, pH 7.4), resuspended, and plated out on 35 mm culture dishes (Falcon, type 3001, Corning Inc., USA) that had previously been pre-incubated overnight with CCT medium plus 4% (v/v) FCS. Non-adherent cells were removed by changing the medium after 1 h (Schreckenberg et al., 2015).

Transferring a complex in vivo situation to an in vitro model is often a major challenge, especially with regard to the concentrations of the applied active ingredients. In this study, the amount of mRNA used was calculated from the lipid concentration detected in the rat heart 2 h after injection of 50 µg [^{3}H]-labelled LNP mRNA. The lipid equivalent of 1.4 µg per gram of cardiac tissue corresponds to approximately 3% at the applied LNP amount of 50 µg. Consequently, 10 µl (≙ 1.0 µg RNA ml^{-1}) or 3.3% of a regular inoculation dose of BNT162b2 (300 µl per dose) or 16.6 µl (≙ 3.3 µg RNA ml^{-1}) of an inoculation dose of mRNA-1273 (500 µl per dose) was applied to the culture dishes, each of which contained 1 ml of cell culture medium (≙ approximately 1 g) (SARS-CoV-2 mRNA Vaccine, report number: 185350). The culture dishes of the respective control groups were not treated.

All cell culture work, including the application of mRNA-1273 and BNT162b2, was performed separately from the subsequent analysis, using different lab space and personnel. Accordingly, all experiments were performed in a blinded manner, without knowledge of the group affiliation of each culture dish.

2.2 | Determination of cell contraction

Absolute and relative cell shortening as well as parameters of contraction dynamics were determined on isolated cardiomyocytes using the 'Cell-Edge Detection System'. In the electric field set up by two AgCl electrodes, the cells were made to contract by successive square-wave pulses (20 V) of opposite polarity (Schreckenberg et al., 2015).

A total of n = 1161 cells from n = 6 or n = 8 independent cell preparations were measured and analysed (see legend to Figure 2 for more details regarding the number of cells and rats). At a stimulation frequency of 2 Hz, a contraction was recorded every 15 s for 1 min using a 500 Hz line scan camera. The average of these four individual measurements represents the contraction of the cell. The cardiomyocytes of a further n = 32 culture dishes from n = 8 independent experiments could not be measured or evaluated at 48 h after application of mRNA-1273 in the two concentrations 1.0 and 3.3 $\mu g \cdot ml^{-1}$ of mRNA, because the cell pattern was predominantly characterized by arrhythmic and irregularly contracting myocytes.

Valid measurements can only be obtained from regularly beating cardiomyocytes. The cell boundaries of irregularly contracting myocardial cells are not properly detected by our system. Arrhythmically beating cells do not provide consistent values within the four contractions recorded per cell (and these values are in some cases non-physiological).

2.3 | Visualization of calcium transients

For the analysis of calcium transients, myocytes were plated out on 35 mm glass-bottomed cell culture dishes (CELLview #627861, Greiner Bio-One International GmbH, Germany) following isolation. Fifty micrograms of Fluo-4, AM (membrane-permeable, excitation at 488 nm, emission at 520 nm, Invitrogen™, USA) were first dissolved in 200 µl DMSO and then diluted 1:200 in a CCT cell culture medium. Immediately before measurement, cells were loaded with Fluo-4 via medium exchange for 10 min at 37°C, washed, and allowed to contract at a stimulation frequency of 2 Hz. Calcium transients were visualized using ION Optix imaging systems (IonOptix LLC, USA).

2.4 | Phalloidin staining protocol

Imaging of the sarcomere structure of isolated cardiomyocytes was performed by confocal laser scanning microscopy for filamentous actin (F-actin). Phalloidine tetramethylrhodamine B isothiocyanate (phalloidin-TRITC, sc-301530, Santa Cruz Biotechnology, Inc., USA) was used, which exhibits an emission maximum of 570–573 nm after

excitation at wavelengths of 540–545 nm, giving the labelled F-actin an orange-red appearance. Cell fixation with 4% paraformaldehyde was followed by incubation with 0.2% Triton-X-100 and then staining with 100 µmol·L^{-1} Phalloidin-TRITC. For morphological assessment, images of three independent cell preparations and three culture dishes per experimental condition were obtained using the Axiovert 200 confocal laser microscope (Carl Zeiss AG, Germany). All histological assessments were performed without knowledge of the treatments of the samples (blindly).

2.5 | Measurement of PKA activity

PKA activity in the cell lysate of isolated cardiomyocytes was measured using the 'PKA (Protein Kinase A) Colorimetric Activity Kit' (#EIAPKA, Invitrogen™, USA). The cells were lysed and harvested exactly according to the manufacturer's instructions. The sample material was then prepared for analysis using an ELISA reader. Set to the recommended parameters, a Tecan Infinite M200 (Tecan Group Ltd., Switzerland) and the associated Tecan i-control software were used to quantify PKA activity.

2.6 | Langendorff perfusion

The clearance of mRNA-1273 and BNT162b2 from coronary vessels into the myocardium and into myocytic and non-myocytic cells was studied ex vivo in isolated perfused hearts of 3-month-old male Wistar rats. Flow-constant perfusion was performed retrogradely via a 16-gauge aortic cannula using Krebs–Henseleit solution, gassed with carbogen (95% O_2, 5% CO_2) and warmed to 37°C. Initially, the coronary flow (≈ 6 ml·min^{-1}) was adjusted to obtain a perfusion pressure of 40 mmHg. Heart rate (approx. 260 bpm), left ventricular pressure (approx. 80-100 mmHg), and aortic pressure (approx. 40-50 mmHg) were recorded continuously. After functional stabilization, the hearts were first perfused with either mRNA-1273 or BNT162b2 for 2 h in a recirculating fashion and then flushed with an open circuit for 15 min. The hearts of the respective control groups were perfused with Krebs–Henseleit buffer only, according to an identical protocol.

PCR-based detection of the respective mRNA was performed either directly on left or right ventricular tissue, septum, and atria, or on cardiomyocytes and non-myocytes isolated according to the protocol described above (see Section 2.1), directly following Langendorff perfusion (Schreckenberg et al., 2015).

A total of n = 16 Langendorff hearts were perfused and data are shown in Figure 6. In Figure 6a, data shown are from n = 2 controls, n = 2 mRNA-1273 and n = 2 BNT162b2. For each heart, PCR-based mRNA detection was performed in n = 8 different regions. All PCRs were performed in duplicate. In Figure 6b, results shown are from n = 2 controls, n = 2 mRNA-1273 (1:2000), n = 2 mRNA-1273 (1:4000), n = 2 BNT162b2 (1:2000) and n = 2 BNT162b2 (1:4000): Myocytes and non-myocytes were isolated/separated from each heart. Thus, mRNA uptake was examined in duplicate in n = 4 myocyte fractions and n = 4 non-myocyte fractions from mRNA-1273 and BNT162b2 perfused hearts, respectively. All treatment groups provided consistent results, so in accordance with the 3Rs Guidelines, we saw no need to add more hearts to the group size.

2.7 | PCR-based detection of mRNAs

Complete RNA was isolated from rat cardiac tissue and isolated cells, and from AC16 cardiomyocytes using TRItidy G™ (A4051, AppliChem GmbH, Germany) following the manufacturer's protocol. After incubation with 1 U DNase per µg RNA for 15 min at 37°C, cDNA synthesis was performed using SuperScript™ III reverse transcriptase (#18080093, Invitrogen™, USA). All PCRs were performed with the CFX Connect Real-Time PCR Detection System (Bio-Rad Laboratories, Inc., Germany) using iQ™ SYBR® Green Supermix (Bio-Rad Laboratories, Inc., Germany).

The primers used were constructed based on the sequences published by Jeong et al. (2021). The following primer pair was used to detect mRNA-1273: Forward: GCCTACAGCAACAACAGCAT, Reverse: TTGAACAGCAGGTCCTCGAT, Product Size: 356 bp; for the detection of BNT162b2: Forward: GGATCCTCTGAGCGAGACAA, Reverse: ACAGGTCGTTCAGCTTGGTA, Product Size: 293 bp.

2.8 | SARS-CoV-2 rapid test

Qualitative detection of the spike protein encoded by mRNA-1273 and BNT162b2 was performed using the Koch Antigen Rapid Test NCV10 (Koch Biotechnology Co., Ltd., China), which specifically and exclusively detects the SARS-CoV-2 spike (S) glycoprotein. With the exception of sample preparation, the test was performed according to the prescribed protocol. For the detection of the spike protein in the cell culture medium, 30 µl supernatant was pipetted onto the corresponding field of the test strip. For intracellular detection, cells were washed with PBS after complete removal of the CCT medium and harvested in 100 µl of lysis buffer (Cell Lysis Buffer #9803, Cell Signaling Technology, Inc., USA). Immediately afterwards, the test was performed with 30 µl of native cell lysate.

2.9 | AC16 human cardiomyocyte cell line

Human AC16 cardiomyocytes (Cat #SCC109, Lot: RD1606008, Merck KGaA, Germany) were cultured on 100 mm dishes (Falcon, type 3003, Corning Inc., USA) in Dulbecco's Modified Eagle's Medium (D6429, EMD Millipore Corp., USA) supplemented with 12.5% heat-inactivated FBS (35–079-CV, Corning Inc., USA) and under 1% antibiotic-antifungal cover (30-004-CI, Corning Inc., USA) according to protocol (#SCC109, EMD Millipore Corp., USA). All AC16-based experiments in this study were performed on cells previously transferred to 60 mm culture dishes

(Falcon, type 3002, Corning Inc., USA). Independent confirmation of all test results for spike protein was performed using the Vazyme antigen detection kit (#C8602C, spike protein recognition regions: aa345-410 and aa420-450, Nanjing Vazyme Medical Technology Co., Ltd., China).

We used AC16 cells to demonstrate both uptake of the LNP-mRNA complexes and translation of the encoded spike protein. Specific detection of the respective mRNA was performed 15, 30, 60, and 90 min after application of mRNA-1273 or BNT162b2 in the three series of experiments listed. Subsequently, spike protein was detected every other day in the cell fraction and supernatant on a total of $n = 5$ control dishes, $n = 5$ mRNA-1273, and $n = 5$ BNT162b2 dishes, respectively, resulting in 90 samples analysed in the three series.

2.10 | Data and statistical analysis

The data and statistical analysis comply with the recommendations of the *British Journal of Pharmacology* on experimental design and analysis in pharmacology. All data are expressed as box and whisker plots. The boxes represent the lower quartile (Q1), the median, and the upper quartile (Q3); whiskers indicate the 1.5 times interquartile range (IQR). An outlier is defined as a number which is less than Q1 or greater than Q3 by more than 1.5 times the IQR. All outliers were included in the statistical analysis. First, data were tested using the non-parametric Kruskal–Wallis test with subsequent pairwise Wilcoxon-Tests for independent data and Bonferroni–Holm *P*-value adjustment for multiple testing. A *P*-value less than 0.05 was considered to be statistically significant.

Because of the exploratory study design in combination with a hypothesis-free study approach, an a priori case number calculation was not performed. The estimation of the required number of independent cell preparations (≙ the number of required experimental animals) was based on our long-term experience regarding the cultivation and functional characterization of cardiomyocytes isolated from adult rat hearts (Schreckenberg et al., 2004).

2.11 | Materials

Isoprenaline (Cat #I5627) was supplied by Merck KGaA, Germany. Both, mRNA-1273 (Spikevax, Moderna) and BNT162b2 (Comirnaty, Pfizer/Biontech) were obtained from a local Government vaccine distribution point.

2.12 | Nomenclature of targets and ligands

Key protein targets and ligands in this article are hyperlinked to corresponding entries in http://www.guidetopharmacology.org, and are permanently archived in the Concise Guide to PHARMACOLOGY 2021/22 (Alexander, Christopoulos et al., 2021; Alexander, Fabbro, et al., 2021; Alexander, Kelly et al., 2021; Alexander, Mathie et al., 2021).

3 | RESULTS

3.1 | The effects of mRNA-1273 and BNT162b2 on the function of left ventricular myocytes 24 and 48 h after application

The function of cardiomyocytes was characterized at a beating frequency of 2 Hz by determining its relative cell shortening (dL/L in %), contraction velocity, and relaxation velocity ($\mu m \cdot s^{-1}$).

After 24 h, cells treated with mRNA-1273 or BNT162b2 did not differ functionally (see Figure 2a–c) or morphologically (see Figure 3a) from untreated control cells.

However, 48 h after application of mRNA-1273, quantification of contraction parameters was no longer possible, since the cell pattern was predominantly characterized by arrhythmic as well as irregular, partially 'peristaltic' contracting myocytes (see Video S1A–F). Regular contractile activity could be recorded in a sufficient number of cardiomyocytes only when the mRNA concentration was reduced to 0.3 $\mu g \cdot ml^{-1}$ of culture medium. Although relative cell shortening was not affected, there was significant deterioration in both dynamic functional parameters (see Figure 2d–f).

In contrast, BNT162b2-treated cells contracted rhythmically and uniformly but, compared with control myocytes, exhibited both a significant increase in relative cell shortening (+22.6%) as well as contraction (+31.9%) and relaxation velocity (+32.1%). With application of 3.3 times the dose of BNT162b2 (BNT162b2 [3.3 μg]), the mRNA concentration per dish was approximately the same as 1× dose of mRNA-1273. Although this dose enhanced the effects already mentioned (cell shortening: +34.6%, contraction velocity: +51.4%, and relaxation velocity: +54.8% vs. control), the characteristic mRNA-1273 symptomatology was not observed (see Figure 2d–f).

The contraction behaviour of BNT162b2-treated cells that developed 24 to 48 h after application was largely consistent with the functional changes that cardiomyocytes (or myocardium) exhibit as a result of catecholamine stimulation. In our model, nearly identical functional parameters could be obtained in untreated cardiomyocytes that received acute treatment with the **β-adrenoceptor** agonist **isoprenaline** (10 $nmol \cdot L^{-1}$ final concentration) after 48 h (see Figure 2d–f).

3.2 | The 'functional state' of isolated cardiomyocytes after 24, 48, and 72 h incubation with mRNAs

Figure 3 illustrates the (functional) state of the cardiac muscle cells over time and in relation to the particular experimental condition. At 24 h (see Figure 3a), the untreated controls and the mRNA-1273/BNT162b2-incubated culture dishes showed regularly contracting cells (percentages of 75% and 77%, respectively). After 48 h (see Figure 3b), the number of contracting myocytes

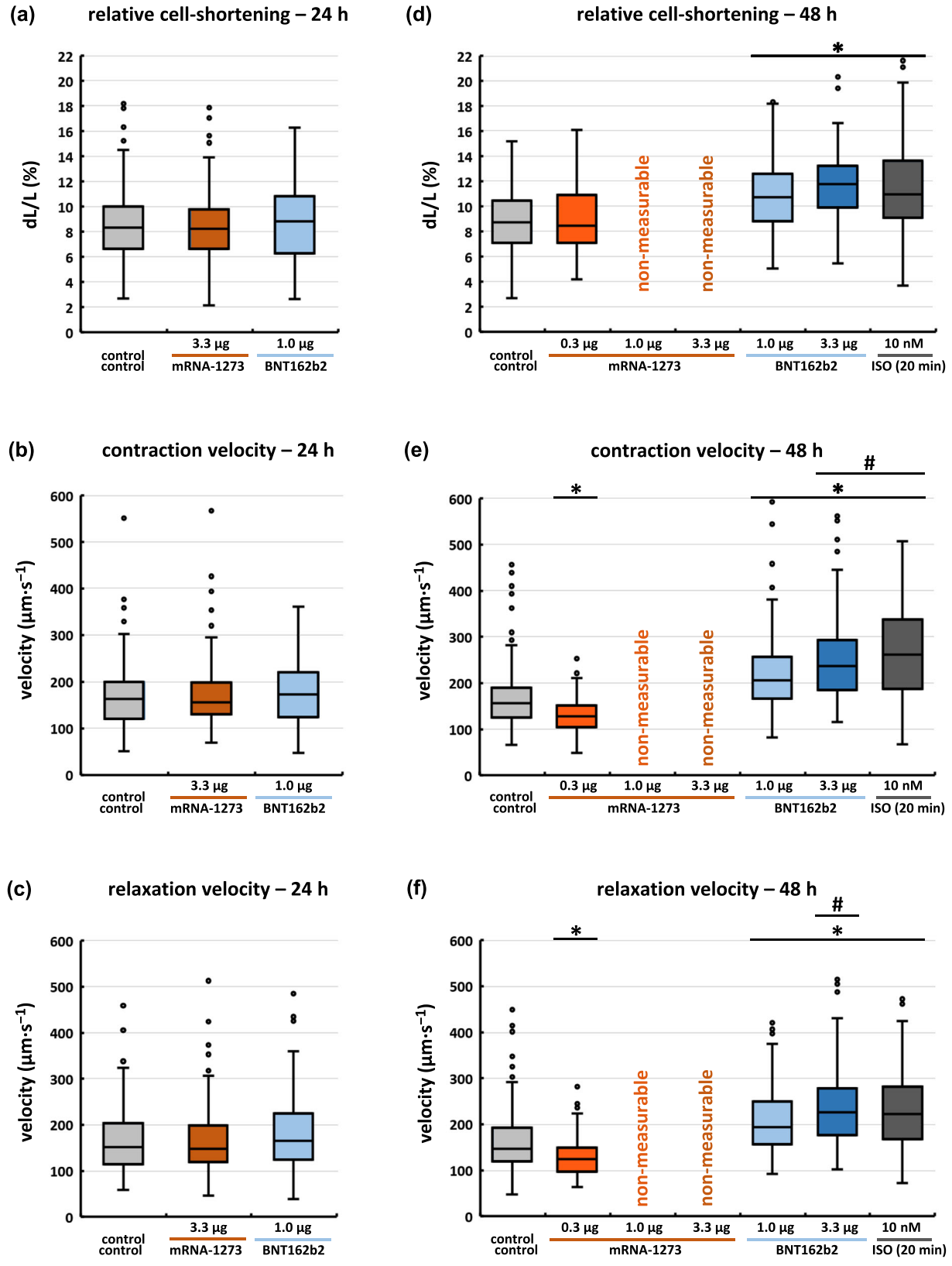

FIGURE 2 Legend on next page.

decreased, and the proportion of non-beating but morphologically intact myocytes and the proportion of rounded or hypercontracted cells increased. In all of the above categories, controls and BNT162b2-treated cells were not significantly different. By contrast, the proportion of regularly contracting myocardial cells was reduced to 10% by the application of mRNA-1273, and arrhythmic as well as irregularly beating cells together accounted for approximately 52% of total cells.

Our model of isolated rat cardiomyocytes allows accurate quantification of myocyte contraction parameters up to 48 h after isolation. After 72 h (see Figure 3c), the 'functional state' was therefore assessed solely in a qualitative fashion. Compared to the control dishes, which still had a 41% share of contracting cardiomyocytes, the cells incubated with mRNA-1273 almost completely ceased to function. In cultures incubated with BNT162b2, the proportion of beating myocytes was reduced to 27%. Incubation with either mRNA also resulted in a significantly increased proportion of rounded or hypercontracted cells.

Reducing the mRNA-1273 dose to 1.0 μg RNA per ml did not improve the previously described symptomatology over time. By contrast, a further decrease to 0.3 $\mu g \cdot ml^{-1}$ significantly increased the proportion of regularly contracting myocardial cells, but was only transiently effective within the first 48 h (see Figure 3d).

3.3 | The effects of mRNA-1273 and BNT162b2 on the calcium transients in isolated cardiomyocytes

In order to visualize calcium transients, cells from all three treatment groups were loaded with Fluo-4 AM for 10 min after 48 h incubation and then electrically stimulated at 2 Hz.

In untreated control myocytes and in BNT162b2-treated cells, both the systolic release and diastolic decrease of calcium were rhythmically and uniformly detectable over the entire cross-sectional area of the respective cell. The calcium cycles of mRNA-1273-treated cardiomyocytes showed arrhythmic as well as localized and irregular transients, which must be interpreted as correlates of the previously described dysfunctions (see Video S2A–G).

The BNT162b2-induced increase in all contraction parameters causally underlies a significant increase in PKA activity (see Section 3.5), leading to increased intensity and dynamics of calcium transients in BNT162b2-treated myocytes.

3.4 | Detection of an intact sarcomere structure using phalloidin staining

Especially with regard to the irregular contractions induced by mRNA-1273, structural damage within the sarcomere structure could not be ruled out. After 48 h of incubation, cells from three preparations were examined for the regular arrangement of their transverse striations by phalloidin staining (see Figure 4). Characteristic, clustered irregularities in the structure of the parallel myofibrils could not be observed in any treatment group; thus, an assignment to the three experimental conditions was not possible via the assessment of the histological preparations.

3.5 | The effects of mRNA-1273 and BNT162b2 on PKA activity after 48 h of incubation

The maintenance as well as the demand-responsive adaptation of cardiac function are primarily under the control of β-adrenoceptors, which regulate the activity of **adenylyl cyclase** and thus the level of **cAMP**, by means of Gs protein. Both positive inotropic and positive lusitropic effects are mediated by cAMP-dependent activation of PKA.

Functionally, incubation with BNT162b2 for 48 h in the absence of extracellular agonists of the β-adrenoceptor significantly increased the relative cell shortening, and the contraction and relaxation rates. Consequently, myocyte PKA activity was determined by ELISA (see Figure 5), and found to increase after 48 h in BNT162b2-treated cells, to levels comparable to those in untreated cells that had received acute β-adrenoceptor stimulation with isoprenaline (10 $nmol \cdot L^{-1}$ final concentration) after 48 h. While mRNA-1273 had no effect on PKA activity, BNT162b2 (3.3 μg) led to a further increase – which, however, comparable to the functional effects, was not proportional to the dose increase.

3.6 | Uptake of mRNA and production of spike protein in rat cardiomyocytes

PCR-based detection of mRNA was conducted to investigate the incorporation of LNP-mRNA complexes in cardiac tissues and ventricular cells. After 2 h perfusion of Langendorff hearts with mRNA-1273

FIGURE 2 Functional analysis of isolated cardiomyocytes: After 24 (a–c) and 48 h (d–f), the effect of mRNA-1273 and BNT162b2 on relative cell shortening (dL/L in %), contraction velocity, and relaxation velocity ($\mu m \cdot s^{-1}$) was examined. mRNA-1273: At 48 h, we could only obtain valid functional data after reducing the concentration of mRNA to 0.3 $\mu g \cdot ml^{-1}$; for technical reasons, regular contraction parameters could no longer be recorded on the predominantly arrhythmic and irregularly contracting myocytes after application of 1.0 and 3.3 μg of mRNA per ml. BNT162b2 (3.3 μg): 3.3-fold dose of BNT162b2 (equivalent to 1× dose of mRNA-1273) was used to investigate the possible relationship between applied mRNA concentration and cardiac symptoms. The application of the non-selective β-adrenoceptor agonist isoprenaline (ISO; 10 nM) for 20-min, causes functionally comparable effects to the 48-h incubation with BNT162b2. Number of measured cells: a–c: n = 171 cells from n = 8 independent preparations; d–f: n = 144 cells from n = 8 (control, mRNA-1273 (0.3 μg–3.3 μg), BNT162b2 (1.0 μg)) and n = 108 cells from n = 6 (BNT162b2 (3.3 μg), ISO (10 nM) independent preparations. *P < 0.05, significantly different from control, #P < 0.05, significantly different from BNT162b2 (1.0 μg).

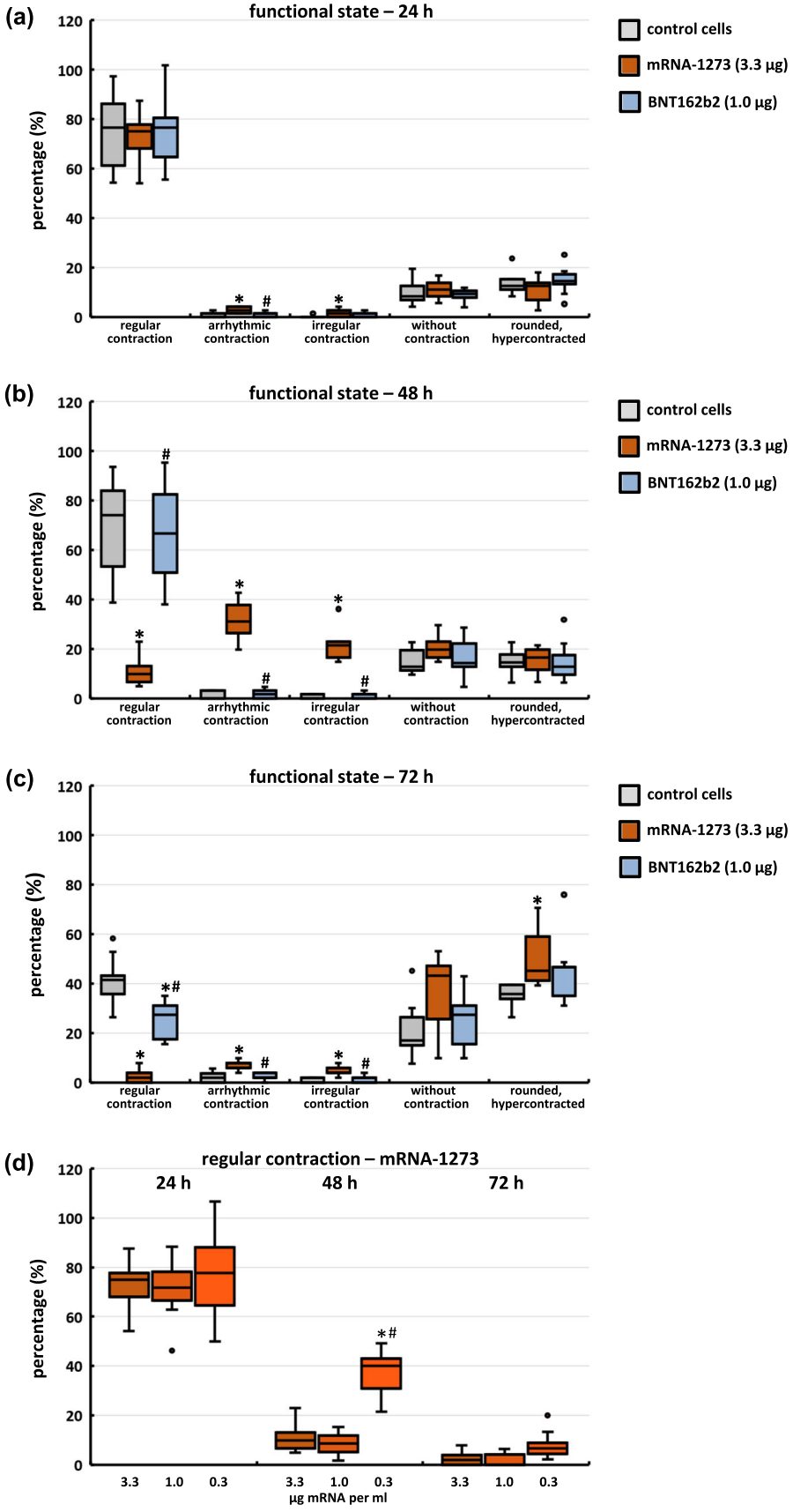

FIGURE 3 The functional state of isolated cardiomyocytes after culture for (a) 24, (b) 48, and (c) 72 h. The evaluation is based on three independent preparations. Cardiomyocytes from nine culture dishes per experimental condition and time point were stimulated by electric field at 2 Hz and assigned to the five criteria in a blinded fashion. Identical visual fields were counted; number of cells evaluated: control/mRNA-1273/BNT162b2; 24 h: 647/648/681; 48 h: 558/548/567; 72 h: 478/458/462. **P* < 0.05, significantly different from control cells, #*P* < 0.05, significantly different from mRNA-1273 (3.3 µg). Panel (d) plots over time the percentage of regularly contracting cardiomyocytes considering the three mRNA-1273 concentrations used. Number of cells evaluated after incubation with mRNA-1273: 3.3 µg/1.0 µg/0.3 µg; 24 h: 648/698/686; 48 h: 548/527/581; 72 h: 458/432/403. **P* < 0.05, significantly different from mRNA-1273 (3.3 µg), #*P* < 0.05, significantly different from mRNA-1273 (1.0 µg).

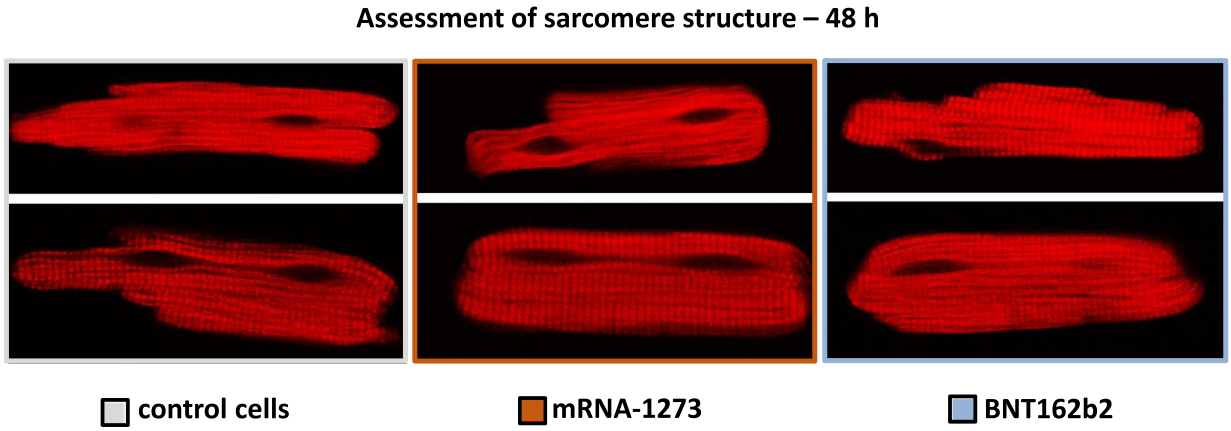

FIGURE 4 Assessment of sarcomere structure using phalloidin staining. After 48 h of culture, isolated cardiomyocytes from three culture dishes per experimental condition from three independent preparations were examined for regular transverse striation. Microscopically visible structural damage was not caused by either mRNA-1273 or BNT162b2.

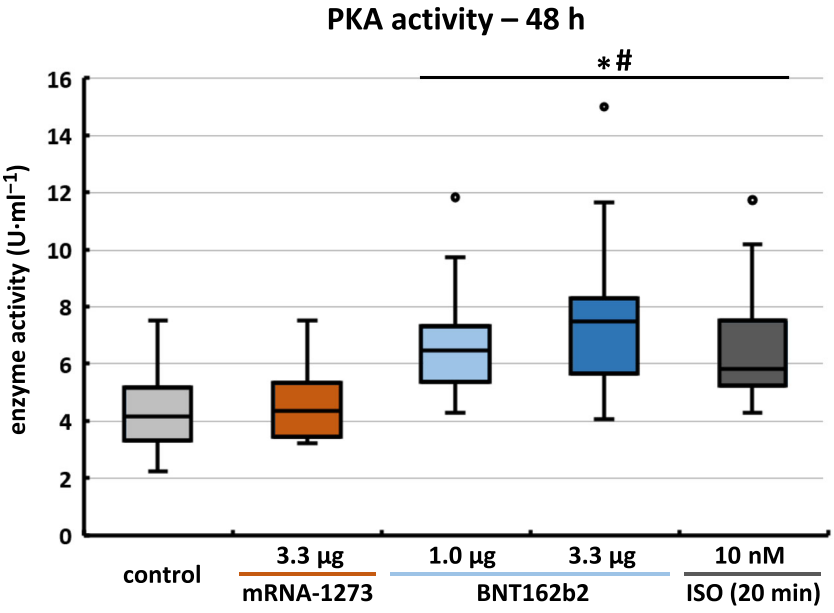

FIGURE 5 ELISA-based determination of PKA activity in myocytes. In contrast to mRNA-1273, BNT162b2 causes a significant increase in PKA activity after 48 h of incubation. Comparable enzyme activity could be obtained by stimulating cardiomyocytes with isoprenaline (ISO; 10 nM final concentration) for 20 min. Data are based on n = 18 [control, ISO (10 nM)] and n = 16 [mRNA-1,273 (3.3 µg), BNT162b2 (1.0 µg, 3.3 µg)] culture dishes from n = 8 independent preparations. *P < 0.05, significantly different from control, #P < 0.05, significantly different from mRNA-1273 (3.3 µg).

or BNT162b2, respectively, and a 15-min washout period, mRNA could be detected in all sections of the left and right ventricular myocardium, in the septum, and in both atria (see Figure 6a). Following cell isolation, we found cell-specific uptake in cardiomyocytes as well as in non-myocytic cells, such as endothelial cells and fibroblasts. In a direct comparison, the cell fraction of non-myocytic cells showed consistently higher levels of mRNA compared to the myocyte fraction after perfusion with either mRNA-1273 or BNT162b2, for both concentrations used (1:2000 and 1:4000) (see Figure 6b).

Under duplicate measurement, all Langendorff hearts gave concordant results with respect to mRNA uptake. Neither mRNA-1273 nor BNT162b2 had any effect on cardiac function or haemodynamics during 2 h of perfusion (data not shown).

The Koch NCV10 rapid antigen assay, which is designed for specific detection of the SARS-CoV-2 spike (S) glycoprotein, was used to monitor the translation of the vaccine-encoded spike protein. Twenty-four hour after incubation of isolated cardiomyocytes with mRNA-1273 or BNT162b2, spike protein was not detectable in the cell lysate or cell culture medium. After 48 h, positive test results were obtained exclusively for the intracellular fraction of mRNA-1273 and BNT162b2 treated cells, with the supernatant always remaining 'negative' (see Figure 6c). Because of the rapid and simple assay procedure, successful translation after application of the two mRNAs was verified by random sampling in all previously described experiments. The rate for positive protein detection was 100% for both mRNA-1273 and BNT162b2 after 48 h of incubation.

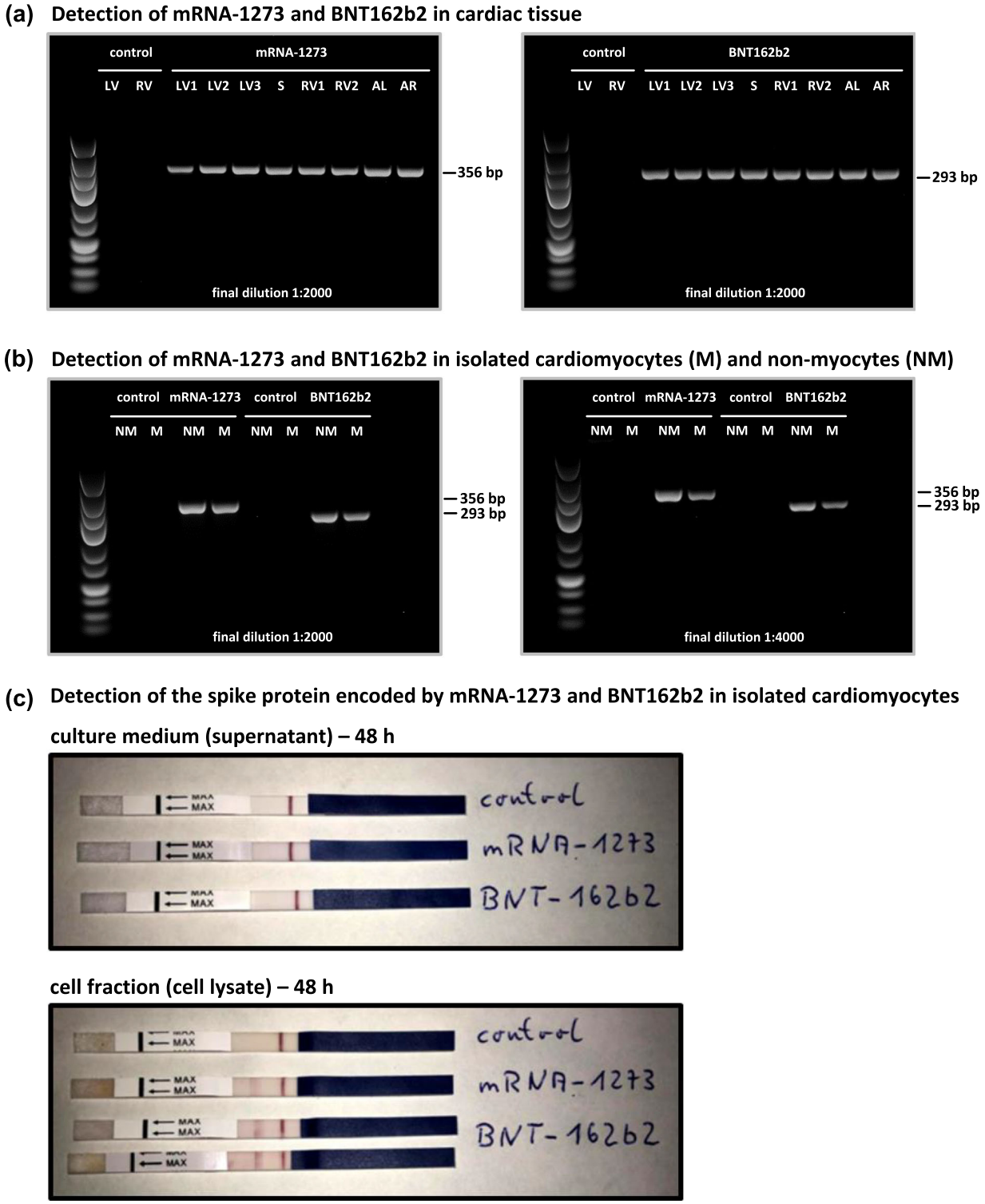

FIGURE 6 Cellular uptake of mRNA and production of spike protein in rat cardiomyocytes. PCR-based detection of mRNA-1273 and BNT162b2 after 2 h Langendorff perfusion was performed in (a) cardiac tissue and (b) cardiomyocytes (M) and non-myocytic cells (NM) isolated immediately after perfusion (n = 2 hearts per experimental condition; mRNA-1273 and BNT162b2 were added at 1:2000 and 1:4000-fold dilution, respectively). Qualitative detection of SARS-CoV-2 spike (S) glycoprotein was performed using the NCV10 rapid antigen assay from Koch Biotechnology Co. Positive test results could be obtained exclusively in the cell fraction after 48-h incubation with mRNA-1273 or BNT162b2. (c) Negative test result of the culture medium and positive result of the cell fraction (BNT162b2 – top: 1-fold dose; bottom: 3.3-fold dose).

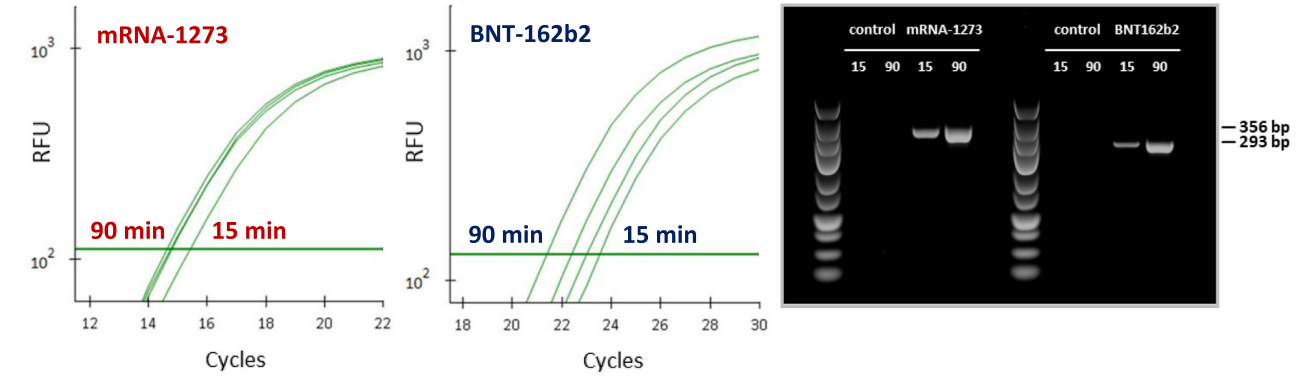

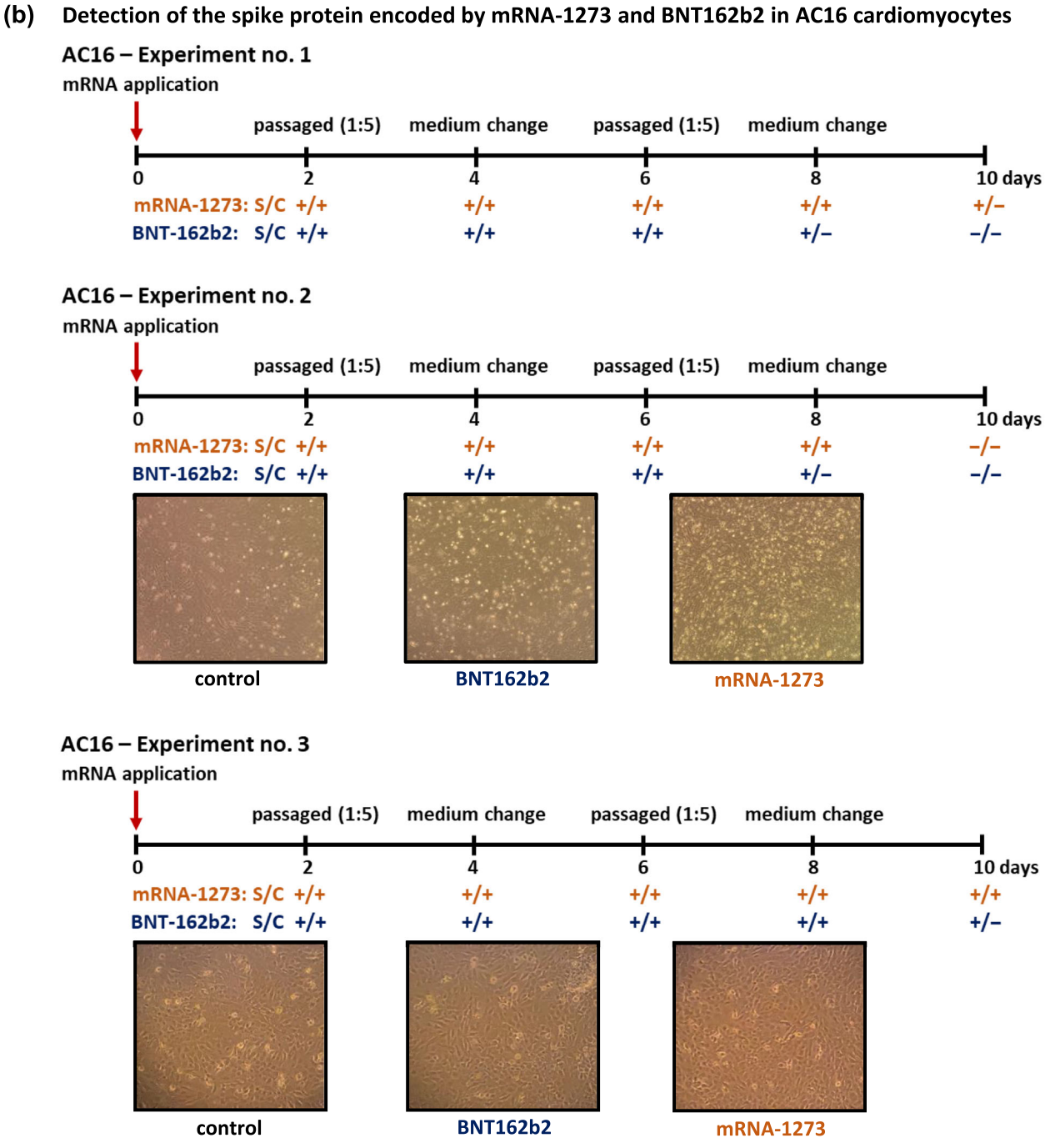

FIGURE 7 Legend on next page.

3.7 | Uptake of mRNA and spike protein production in human AC16 cardiomyocytes

Using the cardiomyocyte cell line AC16, we were able to demonstrate the efficient uptake of LNP-mRNA complexes and the translation of the encoded spike protein in human cells of ventricular origin. Specific detection of the respective mRNA was performed 15, 30, 60, and 90 min after application of mRNA-1273 or BNT162b2 (see Figure 7a). In contrast to the isolated cardiomyocytes of adult rat hearts, the spike protein could be detected in AC16 cultures in both the cell fraction and supernatant. By reducing the RNA concentration used to 0.66 $\mu g \cdot ml^{-1}$ (mRNA-1273) and 0.2 $\mu g \cdot ml^{-1}$ (BNT162b2) in experiment no. 3, the number of positive test results could be increased, due to reduced cell damage in comparison with the first two experiments (see images). In addition, the results regarding the production time of the spike protein must take into account the two cell passages in a ratio of 1:5, so that the positive findings of the last 4 days are mathematically based on only 4% of the originally incubated cells (see Figure 7b).

4 | DISCUSSION

Functionally, in ventricular cardiomyocytes, both mRNA-1273 and BNT162b2 cause characteristic symptoms, each of which is based on independent as well as highly specific pathomechanisms. Whereas mRNA-1273 induces both arrhythmic and irregular contractions via extensive disruption of sarcoplasmic calcium release, BNT162b2 causes a disproportionate increase in cardiomyocyte functional parameters via chronic activation of PKA.

Within the first 24 h after application of the mRNAs, neither functional disturbances nor morphological abnormalities were observed. By contrast, after 48 h, specific symptomatology could be clearly diagnosed for both mRNA-1273 and BNT162b2. As a causal agent, the time kinetics in both cases point to the spike protein, which must first be translated and cytoplasmically enriched in sufficient concentration. Immunological cross-reactions can be excluded by the cell culture model used; direct damage to the cell membrane by the LNP-mRNA complexes would have already become symptomatic after 24 h (Tsilingiris et al., 2022).

The rapid and efficient uptake of LNP-mRNA complexes could be reliably demonstrated in both ex vivo perfused Langendorff hearts as well as in human AC16 cardiomyocytes. While our two cell culture systems do not permit any concrete conclusions regarding the duration or extent of spike protein production, all results for AC16 cells indicate a highly efficient and possibly long-lasting translation.

The spike protein, encoded by both mRNA-1273 and BNT162b2, is stabilized in its prefusion form (S-2P) by double proline substitution at positions 986 and 987. Translation results in proteins with identical amino acid sequences in both cases, but BNT162b2 has 4284 nucleotides, 280 nucleotides more than mRNA-1273; other differences include the design and modifications of the 5′- and 3′-UTRs, codon optimization, and the chemical structure of the LNPs (Granados-Riverona & Aquino-Jarquin, 2021; Xia, 2021). Consequently, post-translational modifications could be responsible for the different pathomechanisms in cardiomyocytes; NMR analyses could be used to identify both structural differences and potential interaction partners.

Regulation of myocardial contraction occurs at the cellular level, primarily by influencing intracellular calcium homeostasis. Voltage-gated **L-type calcium channels** are responsible for the influx of so-called 'trigger calcium' that activates intracellularly located **ryanodine receptors** (RyR2), which subsequently release large amounts of calcium from the sarcoplasmic reticulum (SR). The increase in cytosolic calcium from 10^{-7} $mol \cdot L^{-1}$ to approximately 10^{-5} $mol \cdot L^{-1}$ is almost entirely due to sarcoplasmic calcium and can be viewed as an initial step in the contraction. The magnitude and dynamics of calcium transients are mainly under the control of PKA, which, after stimulation of β-adrenoceptors, regulates the release via phosphorylation of the L-type calcium channel as well as RyR2 and, via phospholamban, the activity of **SERCA2a** and, thus, the return of calcium to the SR (Schreckenberg, 2016).

The arrhythmic as well as completely irregular contractions, together with the irregular as well as localized calcium transients, indicate a significant dysfunction of RyR2, which was induced only after incubation with mRNA-1273. Direct impairment of SR-dependent calcium release would also explain the significantly reduced contractile velocity after application of the reduced mRNA-1273 dose.

As a result of transfection with recombinant SARS-CoV-2 spike protein, Clemens et al. found comparable effects on rhythm and calcium transients in human induced pluripotent stem cell-derived cardiomyocytes (hiPSC-CMs) (Clemens et al., 2023).

Numerous papers have identified mutation-related RyR2 dysfunction as a causal agent of arrhythmias, ventricular tachycardia, and sudden cardiac death (Jóna & Nánási, 2006; Seidlmayer et al., 2018; Sleiman et al., 2021; Thomas et al., 2005). RyR2-induced cardiomyopathies may further be characterized by a structurally remodelled myocardium, but our histological findings did not provide evidence of disruption of sarcomeric transverse striation, so that the described

FIGURE 7 Uptake of mRNA and production of spike protein in human AC16 cardiomyocytes. The amount of mRNA taken up in the cell fraction was determined 15, 30, 60, and 90 min after incubation with mRNA-1273 or BNT162b2. Detection and visualization were performed (a) by real-time PCR and agarose gel. Spike protein could be detected over a period of (b) 6 to 10 days in both the supernatant (S) and the cell fraction (C); release of the spike protein into the cell culture medium was not demonstrated for the isolated rat cardiomyocytes. Reducing the amount of mRNA applied in experiment no. 3 resulted in a prolongation of positive test results due to less cellular damage (see images). mRNA concentration used in experiment no. 1 and no. 2: mRNA-1273 (3.3 $\mu g \cdot ml^{-1}$), BNT162b2 (1.0 $\mu g \cdot ml^{-1}$); experiment no. 3: mRNA-1273 (0.66 $\mu g \cdot ml^{-1}$), BNT162b2 (0.2 $\mu g \cdot ml^{-1}$).

symptomatology 48 h after application is in all likelihood purely functional in causation (Benitah et al., 2021). However, severe dysfunction of isolated cardiomyocytes, regardless of the underlying cause, can cause immediate structural damage in the myocardial cellular complex by mechanical forces on directly adjacent cardiomyocytes (Schauer et al., 2022).

Our results on the effects of BNT162b2 are fully consistent with the pathological findings of Gill et al. (2022), who disagree with the clinical diagnosis of 'classic myocarditis' as a cause of death in both cases examined, by describing the cardiac changes as a consequence of catecholamine-induced toxic cardiomyopathy. Without being able to identify the exact molecular mechanism, incubation with BNT162b2 causes functionally comparable effects to acute stimulation of cardiomyocytes with isoprenaline via an increase in PKA activity. BNT162b2-induced sustained activation of PKA could thus correspond histopathologically to catecholamine-induced cardiomyopathy. The permanent stimulation of β-adrenergic signalling mechanisms not only increases the energy demand of the myocardium; the increase in heart rate simultaneously reduces the diastolic filling time of the coronary arteries, thus also lowering energy supply (Casey et al., 2017; Kassim et al., 2008; Lefkowitz et al., 2000).

Moreover, our present findings contradict the assumption that the high mRNA concentration of an mRNA-1273 vaccine dose is alone responsible for the increased rate of cardiac side-effects. The 3.3-fold dose of BNT162b2 potentiates the previously induced effects of the 1-fold dose, but the symptomatology triggered by mRNA-1273 was not observed, even after application of identical mRNA concentrations. If there is no other common pathomechanism contributing to the cardiac side-effects by differential diagnosis in vivo, the expression or severity of clinical symptoms alone could explain the unequal risk ratio. This assumption is supported by our findings regarding the 'functional state' of the cells 72 h after application. At this time, the proportion of regularly contracting cells was significantly reduced in BNT162b2-incubated cultures, compared with untreated controls, but in the presence of mRNA-1273, cardiomyocytes almost completely ceased to function.

The main experiments in this study were performed on cardiac muscle cells from 3-month-old male Wistar rats. In further studies, we will investigate the influence of age and gender on the described pathomechanisms, and on the evolution and severity of dysfunction (Bugiardini et al., 2023; Ferdinandy et al., 2019; Ferdinandy et al., 2023). In addition, it would be important to determine the influence of mRNA-1273 and BNT162b2 on the function of muscle cells specific to the cardiac conduction system, which are histologically differentiated from working myocardial cells. In these cells, heart rate and conduction velocity are also under the control of PKA, which is able to regulate the level and rate of calcium cycling via its influence on RyR2 and SERCA2a. In the study published by Mansanguan et al., approx. 18% of 301 adolescents aged 13 to 18 years studied developed ECG abnormalities after two doses of BNT162b2 vaccine (Mansanguan et al., 2022).

Contrary to the clinically diagnosed side-effects, which are predominantly classified as myo- and/or pericarditis, both mRNA-based SARS-Cov-2 vaccines induced functional disturbances in isolated cardiomyocytes that correspond pathophysiologically to cardiomyopathy. RyR2 impairment and sustained PKA activation—both of which are attributable to the intracellular interactions of the spike protein—are risk factors for sudden cardiac death, ventricular tachyarrhythmias and contractile dysfunction. Both mechanisms also provide a possible explanation for persistent cardiac symptoms, as observed in the context of long COVID/post-COVID syndrome (Gyöngyösi et al., 2023). Because rodents became susceptible to SARS-CoV-2 with the emergence of the spike N501Y mutation, the rat model offers the advantage of directly comparing the effects of mRNA-based COVID vaccines and the consequences of infection with SARS-CoV-2 at the level of the isolated cardiomyocyte (Shuai et al., 2021).

Our present study has some limitations. Although all of our present findings obtained from isolated perfused hearts and isolated cardiomyocytes indicate the LNPs of both vaccines on their own do not negatively affect cardiomyocyte function or structure, either acutely or within the first 24 h, the effect of control LNPs were not studied here. Unfortunately, LNPs loaded with suitable control mRNA or 'unloaded' LNPs are not currently available for the research community. Accordingly, it is not possible, at this time, to conclusively assess the effects that may be specifically attributable to the nanoparticles themselves.

In conclusion, currently approved SARS-CoV-2 vaccines are effective in preventing COVID-19 and its sequelae, but our present data suggest that the risk–benefit ratio of mRNA-based vaccines should be re-evaluated taking into consideration of current preclinical cardiac safety data that have revealed a hidden cardiotoxic effect of the vaccines. Furthermore, the present findings should be taken into account in future diagnosis and therapy of cardiac symptoms, temporally coincident with mRNA-based COVID vaccination.

DECLARATION OF TRANSPARENCY AND SCIENTIFIC RIGOUR

This Declaration acknowledges that this paper adheres to the principles for transparent reporting and scientific rigour of preclinical research as stated in the *BJP* guidelines for Design & Analysis and Animal Experimentation, and as recommended by funding agencies, publishers and other organizations engaged with supporting research.

AUTHOR CONTRIBUTIONS

Participated in research design: R. Schreckenberg, N. Woitasky, N. Itani, P. Ferdinandy, R. Schulz. *Conducted experiments*: R. Schreckenberg, N. Woitasky, N. Itani, L. Czech. *Performed data analysis*: R. Schreckenberg, N. Itani, R. Schulz. *Contributed to the writing of the manuscript*: All authors.

ACKNOWLEDGMENTS

PF was supported by the National Research, Development and Innovation Office of Hungary [National Heart Laboratory (RRF-2.3.1-

21-2022-00003) and 2020-1.1.6-JÖVŐ-2021-00013 – investment into the future], and by the EU Horizon 2020 project COVIRNA (Grant #101016072). PF is a vice chair of the COST CIG (IG16225) and an MC member of the COST CardioRNA project (CA17129). Open Access funding enabled and organized by Projekt DEAL.

CONFLICT OF INTEREST STATEMENT

No competing financial interests exist.

DATA AVAILABILITY STATEMENT

The data that support the findings of this study are available from the corresponding author upon reasonable request.

REFERENCES

Alexander, S. P., Christopoulos, A., Davenport, A. P., Kelly, E., Mathie, A., Peters, J. A., Veale, E. L., Armstrong, J. F., Faccenda, E., Harding, S. D., Pawson, A. J., Southan, C., Davies, J. A., Abbracchio, M. P., Alexander, W., Al-hosaini, K., Bäck, M., Barnes, N. M., Bathgate, R., … Ye, R. D. (2021). THE CONCISE GUIDE TO PHARMACOLOGY 2021/22: G protein-coupled receptors. *British Journal of Pharmacology*, *178*(S1), S27–S156. https://doi.org/10.1111/bph.15538

Alexander, S. P., Fabbro, D., Kelly, E., Mathie, A., Peters, J. A., Veale, E. L., Armstrong, J. F., Faccenda, E., Harding, S. D., Pawson, A. J., Southan, C., Davies, J. A., Boison, D., Burns, K. E., Dessauer, C., Gertsch, J., Helsby, N. A., Izzo, A. A., Koesling, D., … Wong, S. S. (2021). THE CONCISE GUIDE TO PHARMACOLOGY 2021/22: Enzymes. *British Journal of Pharmacology*, *178*(S1), S313–S411. https://doi.org/10.1111/bph.15542

Alexander, S. P., Kelly, E., Mathie, A., Peters, J. A., Veale, E. L., Armstrong, J. F., Faccenda, E., Harding, S. D., Pawson, A. J., Southan, C., Buneman, O. P., Cidlowski, J. A., Christopoulos, A., Davenport, A. P., Fabbro, D., Spedding, M., Striessnig, J., Davies, J. A., Ahlers-Dannen, K. E., … Zolghadri, Y. (2021). THE CONCISE GUIDE TO PHARMACOLOGY 2021/22: Other Protein Targets. *British Journal of Pharmacology*, *178*(S1), S1–S26. https://doi.org/10.1111/bph.15537

Alexander, S. P., Mathie, A., Peters, J. A., Veale, E. L., Striessnig, J., Kelly, E., Armstrong, J. F., Faccenda, E., Harding, S. D., Pawson, A. J., Southan, C., Davies, J. A., Aldrich, R. W., Attali, B., Baggetta, A. M., Becirovic, E., Biel, M., Bill, R. M., Catterall, W. A., … Zhu, M. (2021). THE CONCISE GUIDE TO PHARMACOLOGY 2021/22: Ion channels. *British Journal of Pharmacology*, *178*(S1), S157–S245. https://doi.org/10.1111/bph.15539

Benitah, J.-P., Perrier, R., Mercadier, J.-J., Pereira, L., & Gómez, A. M. (2021). RyR2 and calcium release in heart failure. *Frontiers in Physiology*, *12*, 734210. https://doi.org/10.3389/fphys.2021.734210

Buchan, S. A., Seo, C. Y., Johnson, C., Alley, S., Kwong, J. C., Nasreen, S., Calzavara, A., Lu, D., Harris, T. M., Yu, K., & Wilson, S. E. (2022). Epidemiology of myocarditis and pericarditis following mRNA vaccination by vaccine product, schedule, and Interdose interval among adolescents and adults in Ontario, Canada. *JAMA Network Open*, *5*, e2218505. https://doi.org/10.1001/jamanetworkopen.2022.18505

Bugiardini, R., Nava, S., Caramori, G., Yoon, J., Badimon, L., Bergami, M., Cenko, E., David, A., Demiri, I., Dorobantu, M., Fronea, O., Jankovic, R., Kedev, S., Ladjevic, N., Lasica, R., Loncar, G., Mancuso, G., Mendieta, G., Miličić, D., … Manfrini, O. (2023). Sex differences and disparities in cardiovascular outcomes of COVID-19. *Cardiovascular Research*, *119*, 1190–1201. https://doi.org/10.1093/cvr/cvad011

Butt, A. A., Omer, S. B., Yan, P., Shaikh, O. S., & Mayr, F. B. (2021). SARS-CoV-2 vaccine effectiveness in a high-risk national population in a real-world setting. *Annals of Internal Medicine*, *174*, 1404–1408. https://doi.org/10.7326/M21-1577

Casey, R. T., Challis, B. G., Pitfield, D., Mahroof, R. M., Jamieson, N., Bhagra, C. J., Vuylsteke, A., Pettit, S. J., & Chatterjee, K. C. (2017). Management of an acute catecholamine-induced cardiomyopathy and circulatory collapse: A multidisciplinary approach. *Endocrinology, Diabetes & Metabolism Case Reports*, *17*, 0122.

Chua, G. T., Kwan, M. Y. W., Chui, C. S. L., Smith, R. D., Cheung, E. C.-L., Ma, T., Leung, M. T. Y., Tsao, S. S. L., Kan, E., Ng, W. K. C., Chan, V. C. M., Tai, S. M., Yu, T. C., Lee, K. P., Wong, J. S. C., Lin, Y. K., Shek, C. C., Leung, A. S. Y., Chow, C. K., … Ip, P. (2022). Epidemiology of acute myocarditis/pericarditis in Hong Kong adolescents following Comirnaty vaccination. *Clinical Infectious Diseases*, *75*, 673–681. https://doi.org/10.1093/cid/ciab989

Clemens, D. J., Ye, D., Zhou, W., Kim, C. S. J., Pease, D. R., Navaratnarajah, C. K., Barkhymer, A., Tester, D. J., Nelson, T. J., Cattaneo, R., Schneider, J. W., & Ackerman, M. J. (2023). SARS-CoV-2 spike protein-mediated cardiomyocyte fusion may contribute to increased arrhythmic risk in COVID-19. *PLoS ONE*, *18*, e0282151. https://doi.org/10.1371/journal.pone.0282151

D'Angelo, T., Cattafi, A., Carerj, M. L., Booz, C., Ascenti, G., Cicero, G., Blandino, A., & Mazziotti, S. (2021). Myocarditis after SARS-CoV-2 vaccination: A vaccine-induced reaction? *The Canadian Journal of Cardiology*, *37*, 1665–1667. https://doi.org/10.1016/j.cjca.2021.05.010

Ferdinandy, P., Andreadou, I., Baxter, G. F., Bøtker, H. E., Davidson, S. M., Dobrev, D., Gersh, B. J., Heusch, G., Lecour, S., Ruiz-Meana, M., Zuurbier, C. J., Hausenloy, D. J., & Schulz, R. (2023). Interaction of cardiovascular nonmodifiable risk factors, comorbidities and comedications with ischemia/reperfusion injury and cardioprotection by pharmacological treatments and ischemic conditioning. *Pharmacological Reviews*, *75*, 159–216. https://doi.org/10.1124/pharmrev.121.000348

Ferdinandy, P., Baczkó, I., Bencsik, P., Giricz, Z., Görbe, A., Pacher, P., Varga, Z. V., Varró, A., & Schulz, R. (2019). Definition of hidden drug cardiotoxicity: Paradigm change in cardiac safety testing and its clinical implications. *European Heart Journal*, *40*, 1771–1777. https://doi.org/10.1093/eurheartj/ehy365

Gill, J. R., Tashjian, R., & Duncanson, E. (2022). Autopsy histopathologic cardiac findings in 2 adolescents following the second COVID-19 vaccine dose. *Archives of Pathology & Laboratory Medicine*, *146*, 925–929. https://doi.org/10.5858/arpa.2021-0435-SA

Granados-Riverona, J. T., & Aquino-Jarquin, G. (2021). Engineering of the current nucleoside-modified mRNA-LNP vaccines against SARS-CoV-2. *Biomedicine & Pharmacotherapy*, *142*, 111953. https://doi.org/10.1016/j.biopha.2021.111953

Gyöngyösi, M., Alcaide, P., Asselbergs, F. W., Brundel, B. J. J. M., Camici, G. G., Martins, P. D. C., Ferdinandy, P., Fontana, M., Girao, H., Gnecchi, M., Gollmann-Tepeköylü, C., Kleinbongard, P., Krieg, T., Madonna, R., Paillard, M., Pantazis, A., Perrino, C., Pesce, M., Schiattarella, G. G., … Davidson, S. M. (2023). Long COVID and the cardiovascular system-elucidating causes and cellular mechanisms in order to develop targeted diagnostic and therapeutic strategies: A joint scientific statement of the ESC working groups on cellular biology of the heart and myocardial and pericardial diseases. *Cardiovascular Research*, *119*, 336–356. https://doi.org/10.1093/cvr/cvac115

Heymans, S., & Cooper, L. T. (2022). Myocarditis after COVID-19 mRNA vaccination: Clinical observations and potential mechanisms. *Nature Reviews. Cardiology*, *19*, 75–77. https://doi.org/10.1038/s41569-021-00662-w

Jeong, D.E., Mccoy, M., Artiles, K., Ilbay, O., Fire, A., Nadeau, K., Park, H., Betts, B., Boyd, S., Hoh, R., & Shoura, M. (2021). Assemblies of

putative SARS-CoV2-spike-encoding mRNA sequences for vaccines BNT-162b2 and MRNA-1273. Available online: https://virological.org/t/assemblies-of-putative-sars-cov2-spike-encoding-mrna-sequences-for-vaccines-bnt-162b2-and-mrna-1273/663

Jóna, I., & Nánási, P. P. (2006). Cardiomyopathies and sudden cardiac death caused by RyR2 mutations: Are the channels the beginning and the end? *Cardiovascular Research*, *71*, 416–418. https://doi.org/10.1016/j.cardiores.2006.06.008

Karlstad, Ø., Hovi, P., Husby, A., Härkänen, T., Selmer, R. M., Pihlström, N., Hansen, J. V., Nohynek, H., Gunnes, N., Sundström, A., Wohlfahrt, J., Nieminen, T. A., Grünewald, M., Gulseth, H. L., Hviid, A., & Ljung, R. (2022). SARS-CoV-2 vaccination and myocarditis in a Nordic cohort study of 23 million residents. *JAMA Cardiology*, *7*, 600–612. https://doi.org/10.1001/jamacardio.2022.0583

Kassim, T. A., Clarke, D. D., Mai, V. Q., Clyde, P. W., & Mohamed Shakir, K. M. (2008). Catecholamine-induced cardiomyopathy. *Endocrine Practice*, *14*, 1137–1149. https://doi.org/10.4158/EP.14.9.1137

Kaya, Z., Leib, C., & Katus, H. A. (2012). Autoantibodies in heart failure and cardiac dysfunction. *Circulation Research*, *110*, 145–158. https://doi.org/10.1161/CIRCRESAHA.111.243360

Khoury, D. S., Cromer, D., Reynaldi, A., Schlub, T. E., Wheatley, A. K., Juno, J. A., Subbarao, K., Kent, S. J., Triccas, J. A., & Davenport, M. P. (2021). Neutralizing antibody levels are highly predictive of immune protection from symptomatic SARS-CoV-2 infection. *Nature Medicine*, *27*, 1205–1211. https://doi.org/10.1038/s41591-021-01377-8

Le Vu, S., Bertrand, M., Jabagi, M.-J., Botton, J., Drouin, J., Baricault, B., Weill, A., Dray-Spira, R., & Zureik, M. (2022). Age and sex-specific risks of myocarditis and pericarditis following Covid-19 messenger RNA vaccines. *Nature Communications*, *13*, 3633.

Lefkowitz, R. J., Rockman, H. A., & Koch, W. J. (2000). Catecholamines, cardiac beta-adrenergic receptors, and heart failure. *Circulation*, *101*, 1634–1637. https://doi.org/10.1161/01.CIR.101.14.1634

Li, C., Chen, Y., Zhao, Y., Lung, D. C., Ye, Z., Song, W., Liu, F. F., Cai, J. P., Wong, W. M., Yip, C. C. Y., Chan, J. F. W., To, K. K. W., Sridhar, S., Hung, I. F. N., Chu, H., Kok, K. H., Jin, D. Y., Zhang, A. J., & Yuen, K. Y. (2022). Intravenous injection of coronavirus disease 2019 (COVID-19) mRNA vaccine can induce acute myopericarditis in mouse model. *Clinical Infectious Diseases*, *74*, 1933–1950. https://doi.org/10.1093/cid/ciab707

Lilley, E., Stanford, S. C., Kendall, D. E., Alexander, S. P. H., Cirino, G., Docherty, J. R., George, C. H., Insel, P. A., Izzo, A. A., Ji, Y., Panettieri, R. A., Sobey, C. G., Stefanska, B., Stephens, G., Teixeira, M. M., & Ahluwalia, A. (2020). ARRIVE 2.0 and the British Journal of Pharmacology: Updated guidance for 2020. *British Journal of Pharmacology*, *177*, 3611–3616. https://doi.org/10.1111/bph.15178

Mansanguan, S., Charunwatthana, P., Piyaphanee, W., Dechkhajorn, W., Poolcharoen, A., & Mansanguan, C. (2022). Cardiovascular manifestation of the BNT162b2 mRNA COVID-19 vaccine in adolescents. *Tropical Medicine and Infectious Disease.*, *7*, 196. https://doi.org/10.3390/tropicalmed7080196

Nyberg, T., Ferguson, N. M., Nash, S. G., Webster, H. H., Flaxman, S., Andrews, N., Hinsley, W., Bernal, J. L., Kall, M., Bhatt, S., Blomquist, P., Zaidi, A., Volz, E., Aziz, N. A., Harman, K., Funk, S., Abbott, S., Hope, R., Charlett, A., … Thelwall, S. (2022). Comparative analysis of the risks of hospitalisation and death associated with SARS-CoV-2 omicron (B.1.1.529) and delta (B.1.617.2) variants in England: A cohort study. *The Lancet.*, *399*, 1303–1312. https://doi.org/10.1016/S0140-6736(22)00462-7

Percie du Sert, N., Hurst, V., Ahluwalia, A., Alam, S., Avey, M. T., Baker, M., Browne, W. J., Clark, A., Cuthill, I. C., Dirnagl, U., Emerson, M., Garner, P., Holgate, S. T., Howells, D. W., Karp, N. A., Lazic, S. E., Lidster, K., MacCallum, C. J., Macleod, M., … Würbel, H. (2020). The ARRIVE guidelines 2.0: updated guidelines for reporting animal research. *PLoS Biol*, *18*, e3000410. https://doi.org/10.1371/journal.pbio.3000410

Racanelli, V., Prete, M., Musaraj, G., Dammacco, F., & Perosa, F. (2011). Autoantibodies to intracellular antigens: Generation and pathogenetic role. *Autoimmunity Reviews*, *10*, 503–508. https://doi.org/10.1016/j.autrev.2011.03.001

SARS-CoV-2 mRNA Vaccine (BNT162, PF-0 7302048): 2.6.5.5B. (n.d.). Pharmacokinetics: organ distribution continued, report number: 185350 page 6. Available at: https://www.pmda.go.jp/drugs/2021/P20210212001/672212000_30300AMX00231_I100_2.pdf

Schauer, J., Buddhe, S., Gulhane, A., Sagiv, E., Studer, M., Colyer, J., Chikkabyrappa, S. M., Law, Y., & Portman, M. A. (2022). Persistent cardiac magnetic resonance imaging findings in a cohort of adolescents with post-coronavirus disease 2019 mRNA vaccine myopericarditis. *The Journal of Pediatrics.*, *245*, 233–237. https://doi.org/10.1016/j.jpeds.2022.03.032

Schreckenberg, R. (2016). Endogenous mechanisms for regulating myocardial contractility. In K.-D. Schlüter (Ed.), *Cardiomyocytes – Active players in cardiac disease* (pp. 135–163). Springer.

Schreckenberg, R., Rebelo, M., Deten, A., Weber, M., Rohrbach, S., Pipicz, M., Csonka, C., Ferdinandy, P., Schulz, R., & Schlüter, K. D. (2015). Specific mechanisms underlying right heart failure: The missing upregulation of superoxide dismutase-2 and its decisive role in antioxidative defense. *Antioxidants & Redox Signaling*, *23*, 1220–1232. https://doi.org/10.1089/ars.2014.6139

Schreckenberg, R., Taimor, G., Piper, H. M., & Schlüter, K.-D. (2004). Inhibition of Ca^{2+}-dependent PKC isoforms unmasks ERK-dependent hypertrophic growth evoked by phenylephrine in adult ventricular cardiomyocytes. *Cardiovascular Research*, *63*, 553–560. https://doi.org/10.1016/j.cardiores.2004.04.032

Seidlmayer, L. K., Riediger, F., Pagonas, N., Nordbeck, P., Ritter, O., & Sasko, B. (2018). Description of a novel RyR2 mutation in a juvenile patient with symptomatic catecholaminergic polymorphic ventricular tachycardia in sleep and during exercise: A case report. *Journal of Medical Case Reports*, *12*, 298. https://doi.org/10.1186/s13256-018-1825-6

Sharff, K. A., Dancoes, D. M., Longueil, J. L., Johnson, E. S., & Lewis, P. F. (2022). Risk of myopericarditis following COVID-19 mRNA vaccination in a large integrated health system: A comparison of completeness and timeliness of two methods. *Pharmacoepidemiology and Drug Safety*, *31*, 921–925. https://doi.org/10.1002/pds.5439

Shuai, H., Chan, J. F., Yuen, T. T., Yoon, C., Hu, J. C., Wen, L., Hu, B., Yang, D., Wang, Y., Hou, Y., Huang, X., Chai, Y., Chan, C. C. S., Poon, V. K. M., Lu, L., Zhang, R. Q., Chan, W. M., Ip, J. D., Chu, A. W. H., … Chu, H. (2021). Emerging SARS-CoV-2 variants expand species tropism to murines. *eBioMedicine*, *73*, 103643. https://doi.org/10.1016/j.ebiom.2021.103643

Sleiman, Y., Lacampagne, A., & Meli, A. C. (2021). 'Ryanopathies' and RyR2 dysfunctions: Can we further decipher them using in vitro human disease models? *Cell Death & Disease*, *12*, 1041. https://doi.org/10.1038/s41419-021-04337-9

Sun, C. L. F., Jaffe, E., & Levi, R. (2022). Increased emergency cardiovascular events among under-40 population in Israel during vaccine rollout and third COVID-19 wave. *Scientific Reports*, *12*, 6978. https://doi.org/10.1038/s41598-022-10928-z

Teo, S. P. (2021). Review of COVID-19 mRNA vaccines: BNT162b2 and mRNA-1273. *Journal of Pharmacy Practice*, *35*, 947–951.

Thomas, N. L., Lai, F. A., & George, C. H. (2005). Differential Ca^{2+} sensitivity of RyR2 mutations reveals distinct mechanisms of channel dysfunction in sudden cardiac death. *Biochemical and Biophysical Research*

Communications, *331*, 231–238. https://doi.org/10.1016/j.bbrc.2005.02.194

Tsilingiris, D., Vallianou, N. G., Karampela, I., Liu, J., & Dalamaga, M. (2022). Potential implications of lipid nanoparticles in the pathogenesis of myocarditis associated with the use of mRNA vaccines against SARS-CoV-2. *Metabolism Open.*, *13*, 100159. https://doi.org/10.1016/j.metop.2021.100159

Tyner, H. L., Burgess, J. L., Grant, L., Gaglani, M., Kuntz, J. L., Naleway, A. L., Thornburg, N. J., Caban-Martinez, A. J., Yoon, S. K., Herring, M. K., Beitel, S. C., Blanton, L., Nikolich-Zugich, J., Thiese, M. S., Pleasants, J. F., Fowlkes, A. L., Lutrick, K., Dunnigan, K., Yoo, Y. M., … Thompson, M. G. (2022). Neutralizing antibody response to pseudotype severe acute respiratory syndrome coronavirus 2 (SARS-CoV-2) differs between mRNA-1273 and BNT162b2 coronavirus disease 2019 (COVID-19) vaccines and by history of SARS-CoV-2 infection. *Clinical Infectious Diseases*, *75*, e827–e837. https://doi.org/10.1093/cid/ciab1038

Vojdania, A., & Kharrazian, D. (2020). Potential antigenic cross-reactivity between SARS-CoV-2 and human tissue with a possible link to an increase in autoimmune diseases. *Clinical Immunology*, *217*, 108480. https://doi.org/10.1016/j.clim.2020.108480

Xia, X. (2021). Detailed dissection and critical evaluation of the Pfizer/BioNTech and Moderna mRNA vaccines. *Vaccines (Basel).*, *9*, 734. https://doi.org/10.3390/vaccines9070734

SUPPORTING INFORMATION

Additional supporting information can be found online in the Supporting Information section at the end of this article.

How to cite this article: Schreckenberg, R., Woitasky, N., Itani, N., Czech, L., Ferdinandy, P., & Schulz, R. (2024). Cardiac side effects of RNA-based SARS-CoV-2 vaccines: Hidden cardiotoxic effects of mRNA-1273 and BNT162b2 on ventricular myocyte function and structure. *British Journal of Pharmacology*, *181*(3), 345–361. https://doi.org/10.1111/bph.16262